

Analysis of Elastic Properties of Polypropylene Composite Materials with Ultra-High Molecular Weight Polyethylene Spherical Reinforcement

Jong-Hwan Yun ¹, Yu-Jae Jeon ² and Min-Soo Kang ^{3,*}

¹ Mobility Materials-Parts-Equipment Center, Kongju National University, Gongju-si 32588, Korea

² Department of Medical Rehabilitation Science, Yeosu Institute of Technology, Yeosu 12652, Korea

³ Division of Smart Automotive Engineering, Sun Moon University, Asan-si 31460, Korea

* Correspondence: kang10101@sunmoon.ac.kr

Abstract: This study proposes an isotropic composite material with enhanced elastic properties based on a reinforcement mechanism using ultra-high molecular weight polyethylene (UHMWPE) spherical molecules. Elastic properties are predicted through finite element analysis by randomly mixing UHMWPE using polypropylene (PP) as a matrix. The change in elastic properties of the composite is calculated for volume fractions of UHMWPE from 10 to 70%. Furthermore, the results of finite element analysis are compared and analyzed using a numerical approach. The results show that the physical properties of the composite material are enhanced by the excellent elastic properties of the UHMWPE, and the finite element analysis results confirm that it is effective up to a volume fraction of 35%.

Keywords: UHMWPE; polypropylene; elastic properties; finite element analysis

Citation: Yun, J.-H.; Jeon, Y.-J.; Kang, M.-S. Analysis of Elastic Properties of Polypropylene Composite Materials with Ultra-High Molecular Weight Polyethylene Spherical Reinforcement.

Materials **2022**, *15*, 5602.

<https://doi.org/10.3390/ma15165602>

Academic Editors: Xuming Xie and Shouke Yan

Received: 24 July 2022

Accepted: 11 August 2022

Published: 15 August 2022

Publisher's Note: MDPI stays neutral with regard to jurisdictional claims in published maps and institutional affiliations.



Copyright: © 2022 by the authors. Licensee MDPI, Basel, Switzerland. This article is an open access article distributed under the terms and conditions of the Creative Commons Attribution (CC BY) license (<http://creativecommons.org/licenses/by/4.0/>).

1. Introduction

A composite material can be defined as an assembly of two or more materials with properties superior to those of each of the constituent materials [1–6]. Composite materials formed by embedding a material in a matrix are commonly called reinforcement arrangements (or fillers) [7–10]. The matrix directly receives the cohesive force and direction of the load. Moreover, the load that the composite material receives may be transmitted as internal stress. A composite material formed in this manner is highly heterogeneous and may be isotropic or anisotropic depending on the material used [11–13]. The properties of the matrix and the charge, shape, proportion of the charge, quality of the interface, and production process used are all parameters that can affect the properties of the composite material [14–17]. In general, a polymer material is most frequently used as the matrix, and various materials such as metal, ceramic, or plastic may be used as the reinforcing material. Such composite materials may exhibit a continuous or discontinuous mechanism according to the shape of the reinforcing material used. A composite mainly formed using fiber as a reinforcing material is an example of a composite material distributed in a continuous phase [18–22]. Continuous phase composite materials are mainly formed by mixing functional fiber material in fiber form with polymer material and are classified as anisotropic due to the directionality of the fiber. To use such anisotropic materials, a fiber-reinforced composite material is configured in a stacked structure to prevent a defect against warpage [23,24]. In contrast, for a composite material with a discontinuous mechanism, the composite is generally manufactured using a spherical additive or an additive in the form of a particle. Additives in a spherical or particle form are freely dispersed in the matrix, and thus, an isotropic composite material can be manufactured [25–29]. Considering such an isotropic

composite material has no directionality, it has a high potential to be widely used in the manufacturing field. In this study, we proposed a composite material using ultra-high molecular weight polyethylene (UHMWPE) spherical particles as the additive to construct such an isotropic composite material.

UHMWPE is attracting significant attention from researchers and industrial engineers owing to its excellent mechanical properties, low density, high chemical resistance and impact strength, low hygroscopicity, and high wear resistance [30–33]. UHMWPE fiber witnessed a surge of research activities right after its commercialization in the late 1970s for a range of applications, including (1) ballistic protection, (2) aerospace, automotive, and defense applications, and, (3) increasingly, medical devices [34–36]. A composite material manufactured by mixing UHMWPE, which has excellent characteristics as an additive, in a polypropylene (PP) matrix would be expected to possess excellent physical properties. In this study, to predict and analyze these properties, a numerical and finite element analysis approach was used to investigate a composite material obtained by mixing UHMWPE with a diameter of 10 μm with PP. In addition, to develop a composite material capable of injection molding, an isotropic composite material is proposed. To develop an isotropic composite material, UHMWPE of a spherical material was used. The physical properties according to the volume fraction (10–70%) of the additive were calculated using micromechanics models (Voigt, Reuss, and Halpin–Tsai) to predict the linear elastic properties of the composite material. Finally, finite element method (FEM) was used to compare and analyze the change in physical properties according to the addition of the UHMWPE spherical particles using the homogenization method.

2. Micromechanics Models

The Voigt model and Reuss model are the two simplest and most classical models used for estimating the elastic modulus of composite materials [37–39]. The rule of mixture predicts the elastic properties of composite materials according to the volume ratio of the constituent materials using Voigt and Reuss models [40–42]. The Voigt and Reuss models are often used to set the bound of the elastic modulus in a composite made of two materials. As the Voigt model is subject to a uniform strain, an upper bound of the elastic modulus can be set. In contrast, the Reuss model may be considered a lower bound because it is subject to uniform stress. As shown in Equation (1), the Voigt model is similar to composite materials connected in series and is developed assuming that the two materials are simply and linearly synthesized according to the volume fraction. E_c is the elastic modulus of the composite material, C_0 is the volume fraction of PP, C_1 is the volume fraction of UHMWPE, E_0 is the elastic modulus of PP, and E_1 is the elastic modulus of UHMWPE. In this formula, $n = 2$ because the synthesized composite material is composed of binary elements.

$$E_c = \sum_{r=0}^n C_r E_r \quad (1)$$

The Reuss constitutive model is used to model elastic plasticity and the total Lagrangian formula is used to model the finite strain. In the Reuss model, the stiffness of the material is generally measured by the elastic modulus E ; in the macroscopic elastic range, stiffness is the force required to cause a unit displacement. Its reciprocal $1/E$ is called compliance, which is the displacement caused by unit force. The Reuss model is presented in Equation (2).

$$E_c = \left(\sum_{r=0}^n C_r \frac{1}{E_r} \right)^{-1} \quad (2)$$

The Halpin–Tsai model is an improvement of the existing mixing law using reinforcement factors calculated through experiments. The reinforcing factor depends on

the shape and arrangement of the additives and the loading conditions. The Halpin–Tsai model [43,44] is applied here to predict the compressive Young's and shear moduli of the composite, which are dependent on the particle volume fraction (PVF). This Halpin–Tsai approach is simple and easy to use in the design process, and the semi-empirical equation can be expressed as Equation (3). ξ is a measure of particle filler that depends on particle geometry. In general, ξ follows Equation (4). Therefore, it has a value of 2 for spherical particles.

$$E_c = \frac{E_0 \cdot [E_1 + \xi \cdot (C_0 \cdot E_0 + C_1 \cdot E_1)]}{C_0 \cdot E_1 + C_1 \cdot E_0 + \xi \cdot E_r} \quad (3)$$

$$\xi = \frac{2l}{d} \quad (4)$$

According to this numerical method, changes in physical properties of the reinforcing material UHMWPE in a PP matrix according to the volume fraction, from 10% to 70% UHMWPE, were calculated.

3. Homogenization Method

In numerical homogenization, it is assumed that the representative volume element (RVE) or unit cell is locally repeated with a very small microstructure compared with the overall macroscopic dimensions of the structure of interest, where the different base materials are fully bonded in the RVE [45]. Computational homogenization methods and their inverse forms with the FEM have been considered to be rather effective for a range of problems [46–48]. Generation of the RVE plays an important role in determining the effective properties of composite materials using finite element techniques using the homogenization method [49]. To implement the finite element analysis modeling required for the homogenization method, UHMWPE was applied to the spherical reinforcing material and assumed to be a sphere with a diameter of 10 μm . The 10 μm UHMWPE powder was studied using PM-200 from MIPELON™. To compare with the experimental results later, a finite element analysis was performed using 10 μm powder. The matrix material was PP, and the RVE was modeled to a size of 40 $\mu\text{m} \times 40 \mu\text{m} \times 40 \mu\text{m}$ in consideration of the size of the reinforcement (Figure 1). In addition, for UHMWPE, an RVE model with irregular culture was used to reflect the characteristics of particles in the hexagonal matrix material. Finite element analysis was conducted to calculate the change in physical properties according to the volume fraction of UHMWPE from 10% to 70% in the PP matrix (Figure 2). The physical properties of PP and UHMWPE used in this study are tabulated in Table 1.

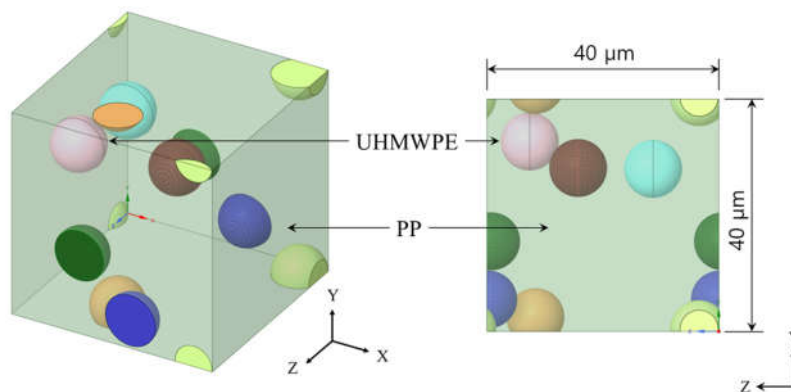
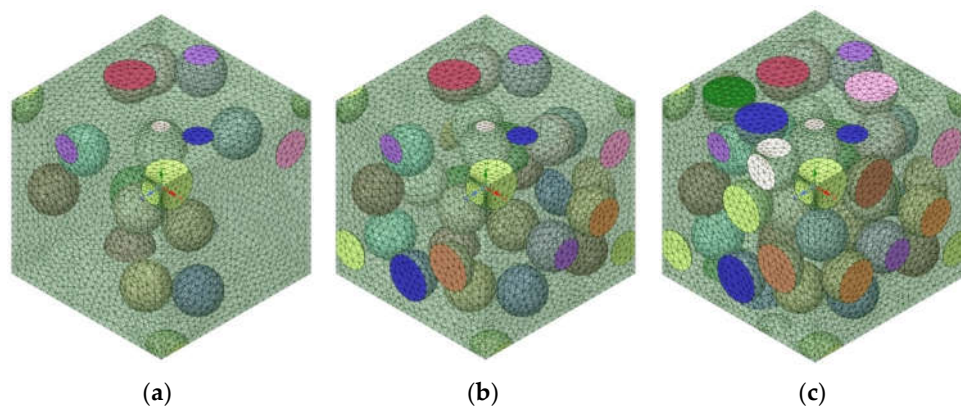


Figure 1. Ultra-high molecular weight polyethylene (UHMWPE) particle-reinforced polypropylene (PP) composite representative volume element modeling.

Table 1. Properties of polypropylene (PP) and ultra-high molecular weight polyethylene (UHMWPE).

No.	Properties	PP	UHMWPE
1	Elastic modulus (MPa)	1325	25,000
2	Shear modulus (MPa)	432.29	10,417
3	Poisson's ratio	0.43	0.20
4	Bulk modulus (MPa)	3154.8	13,889.0
5	Density (kg/m ³)	904	950

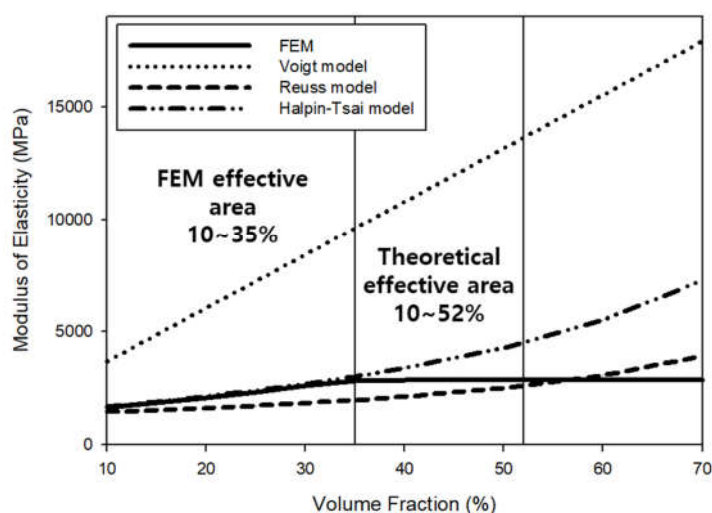
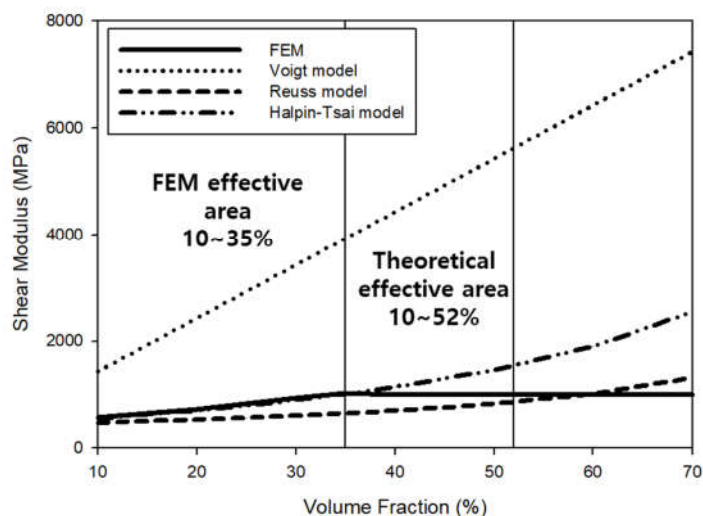
**Figure 2.** Mesh modeling with different ultra-high molecular weight polyethylene (UHMWPE) volume fractions: (a) 10%, (b) 20%, and (c) 30%.

4. Results and Discussion

Table 2 shows the numerical values according to the micromechanics model. In addition, Figure 3 shows changes in the predicted elastic modulus according to the volume fraction. Based on the results of linearly calculating the elastic modulus using the Voigt model, the UHMWPE volume fraction of 10% was calculated to have a value of at most 1798.5 MPa. As a result of analyzing the elastic modulus using the Reuss model, the lowest value was 1350.6 MPa. The elastic modulus calculated using the Halpin–Tsai model was 1394.3 MPa, most similar to the average elastic modulus obtained through the FEM (1394.07 MPa). As the volume fraction linearly increased, the Voigt model elastic modulus linearly increased, and those calculated by the Reuss model and the Halpin–Tsai model also showed a tendency to increase because of the increased influence of the elastic modulus of UHMWPE with an increase in the volume fraction. As shown in Figure 4, similar results were obtained for the predicted shear modulus. Elastic properties, such as elastic modulus and shear modulus, increased as the volume fraction of UHMWPE increased due to the excellent physical properties of UHMWPE (Figures 3 and 4). In general, numerically accessible micromechanics models rely on volume fractions to yield elastic properties. Therefore, theoretically, as the volume fraction of UHMWPE increases, physical properties may be improved [50,51]. Furthermore, the results of predicting the elastic properties of the composite material using the FEM showed a tendency most similar to the elastic modulus and the shear modulus values calculated using the Halpin–Tsai model.

Table 2. Tubular data of micromechanics.

		2%	4%	6%	8%	10%	15%	20%	25%	30%	35%	40%	50%	60%	70%
Voigt model	E	1798.5	2272.0	2745.5	3219.0	3692.5	4876.3	6060.0	7243.8	8427.5	9611.3	10,795.0	13,162.5	15,530.0	17,897.5
	G	632.0	831.7	1031.4	1231.1	1430.8	1930.0	2429.2	2928.5	3427.7	3926.9	4426.2	5424.6	6423.1	7421.6
	nu	0.43	0.42	0.42	0.41	0.41	0.40	0.38	0.37	0.36	0.35	0.34	0.32	0.29	0.27
Reuss model	E	1350.6	1377.2	1404.8	1433.6	1463.6	1544.4	1634.6	1736.0	1850.8	1981.9	2133.0	2516.6	3068.6	3930.6
	G	440.7	449.5	458.7	468.2	478.1	504.9	534.8	568.5	606.8	650.5	701.1	830.1	1017.4	1313.8
	nu	0.42	0.41	0.40	0.39	0.39	0.37	0.35	0.33	0.32	0.31	0.29	0.27	0.25	0.24
Halpin-Tsai	E	1394.3	1466.0	1540.3	1617.3	1697.2	1910.8	2146.4	2407.6	2699.0	3026.0	3395.6	4300.8	5524.7	7271.8
	G	455.7	479.9	505.0	531.1	558.2	630.8	711.2	800.8	901.1	1014.3	1143.0	1461.7	1900.8	2544.0
	nu	0.42	0.42	0.41	0.41	0.40	0.39	0.38	0.36	0.35	0.34	0.33	0.30	0.28	0.26

**Figure 3.** Values of Elastic modulus according to the volume fraction predicted by various models: Voigt, Reuss, Halpin–Tsai, and the finite element method (FEM).**Figure 4.** Values of shear modulus according to the volume fraction predicted by various models: Voigt, Reuss, Halpin–Tsai, and the finite element method (FEM).

As shown in Figure 5, the Poisson's ratio of the PP-UHMWPE composite material calculated by numerical and FEM analysis varied with the volume fraction of composite material formation according to the difference in Poisson's ratio between PP and UHMWPE. The Halpin–Tsai model and the FEM model showed the most similar tendencies in the prediction model for the elastic modulus and the shear modulus, but the FEM did not match any numerical analysis model in the calculation of the Poisson's ratio.

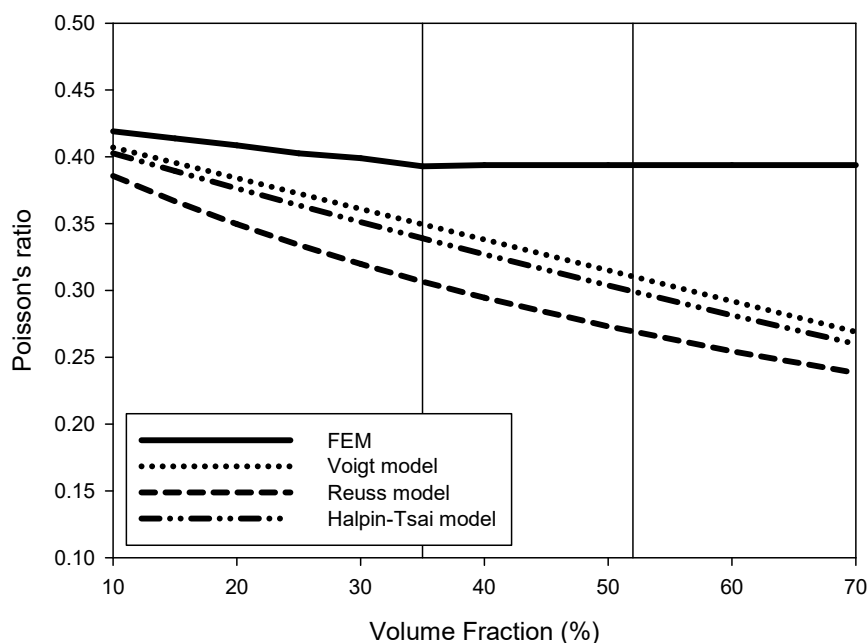


Figure 5. Values of Poisson's ratio according to the volume fraction predicted by various models: Voigt, Reuss, Halpin–Tsai, and the finite element method (FEM).

The size of the RVE used for finite element analysis in this study was $40 \times 40 \times 40 \mu\text{m}$, and the spherical size of UHMWPE was $10 \mu\text{m}$. Therefore, for regularly arranged UHMWPE spheres, up to 64 spheres can theoretically be arranged as presented in Figure 6a, and accordingly, the maximum volume fraction can be expected to be 52%. However, based on the results of calculating the physical properties through the FEM, it was confirmed that the volume fraction of UHMWPE was constant after 35%, as shown in Figures 3–5 because it represents the maximum at a volume fraction of 35%, depending on the batch model of the UHMWPE reinforcing material randomly formed into the RVE lattice. According to the FEM analysis results, when the volume fraction of UHMWPE was 35% or more in the RVE, the spherical UHMWPE additive had directionality caused by overlapping the inner spherical UHMWPE powder as shown in Figure 6b. Therefore, it can be concluded that physical property analysis according to the influence of the tensor should be performed with anisotropic material above 35% volume fraction of UHMWPE. To this end, the elastic modulus and shear modulus of the PP-UHMWPE composite material were found to be similar in the Halpin–Tsai model and the FEM model up to 35% volume fraction of UHMWPE, but the results obtained from the FEM analysis are not valid above 35% volume fraction. Furthermore, it can be determined that the UHMWPE spherical composite material of $10 \mu\text{m}$ can be applied up to the theoretically maximum volume fraction of UHMWPE of 52%. UHMWPE powder of $10 \mu\text{m}$ or less may be used to ensure a higher volume fraction of UHMWPE and thereby enhance physical and elastic properties.

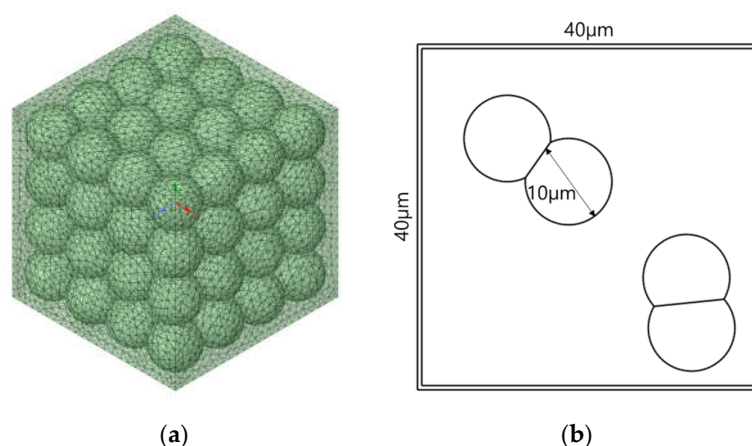


Figure 6. Spherical ultra-high molecular weight polyethylene (UHMWPE) particles at a volume fraction of 35% or more: (a) regular arrangement of spherical UHMWPE and (b) overlapping influence of spherical UHMWPE.

5. Conclusions

In this study, physical properties were predicted using numerical analysis and finite element analysis to predict the elastic properties of composite materials using 10 μm UHMWPE spherical powder as a reinforcing material and PP as a matrix. As spherical powder was used as the reinforcing material, the PP-UHMWPE powder composite could be modeled as an isotropic material. The elastic properties according to the volume fraction of the UHMWPE reinforcing material were compared and analyzed. As numerical methods, the Voigt, Reuss, and Halpin–Tsai models were used, and for the finite element analysis, the homogenization method using RVE identification was used for comparative analysis. The results are as follows.

- (1) The linear calculation according to the volume fraction using the Voigt model was found to be the upper bound of the predicted elastic properties and showed a large error range when compared with the FEM analysis. In the calculation using the Reuss model, the prediction result of elastic properties was lower than that of the FEM analysis. The results of the calculation of elastic properties using the Halpin–Tsai model were found to be most similar to the FEM analysis.
- (2) The powders of the spherical UHMWPE could theoretically be dispersed inside PP at a volume fraction of up to 52% if arranged in a lattice structure. However, in the FEM model, spherical powders of UHMWPE could be dispersed up to 35% volume fraction when they were randomly arranged.
- (3) As a result of comparing and analyzing the numerical finite element analysis results for predicting the elastic properties of PP-UHMWPE isotropic composite materials, it was confirmed that the results of finite element analysis are reliable up to 35% UHMWPE volume fraction and theoretically up to 52%.
- (4) To improve elastic properties, UHMWPE powder of 10 μm or less should be used to form an isotropic composite material by increasing the volume fraction of UHMWPE.

In the future, it is necessary to conduct research to predict the elastic properties of anisotropic composite materials in the high-UHMWPE volume fraction state (55% or more), and there is also a need to study changes in the physical orientation and elastic properties of the composite material according to the overlapping of the spherical UHMWPE powders.

Author Contributions: Conceptualization, J.-H.Y.; Writing—original draft, Y.-J.J.; Writing—review & editing, writing—original draft preparation, supervision, M.-S.K. All authors have read and agreed to the published version of the manuscript.

Funding: This work was supported by National Research Foundation of Korea (NRF) grants funded by the Korea government (MSIT) (No022R1G1A1012340 and No022R1G1A1004962). This research was supported by “Regional Innovation Strategy (RIS)” through the National Research Foundation of Korea(NRF) funded by the Ministry of Education (MOE) (2021RIS-004).

Conflicts of Interest: The authors declare no conflict of interest.

References

1. Dagdag, O.; Safi, Z.; Hsissou, R.; Erramli, H.; EL Bouchti, M.; Wazzan, N.; Guo, L.; Verma, C.; Ebenso, E.E.; Elharfi, A. Epoxy pre-polymers as new and effective materials for corrosion inhibition of carbon steel in acidic medium: Computational and experimental studies. *Sci. Rep.* **2019**, *9*, 11715.
2. Khalil, H.A.; Tehrani, M.; Davoudpour, Y.; Bhat, A.; Jawaid, M.; Hassan, A. Natural fiber reinforced poly (vinyl chloride) composites: A review. *J. Reinf. Plast. Compos.* **2013**, *32*, 330–356.
3. Hsissou, R.; Abbout, S.; Seghiri, R.; Rehioui, M.; Berisha, A.; Erramli, H.; Assouag, M.; Elharfi, A. Evaluation of corrosion inhibition performance of phosphorus polymer for carbon steel in [1 M] HCl: Computational studies (DFT, MC and MD simulations). *J. Mater. Res. Technol.* **2020**, *9*, 2691–2703.
4. Dagdag, O.; Hsissou, R.; El Harfi, A.; Safi, Z.; Berisha, A.; Verma, C.; Ebenso, E.E.; Quraishi, M.A.; Wazzan, N.; Jodeh, S.; et al. Epoxy resins and their zinc composites as novel anti-corrosive materials for copper in 3% sodium chloride solution: Experimental and computational studies. *J. Mol. Liq.* **2020**, *315*, 113757.
5. Hsissou, R.; Dagdag, O.; Abbout, S.; Benhiba, F.; Berradi, M.; El Bouchti, M.; Berisha, A.; Hajjaji, N.; Elharfi, A. Novel derivative epoxy resin TGETET as a corrosion inhibition of E24 carbon steel in 1.0 M HCl solution. Experimental and computational (DFT and MD simulations) methods. *J. Mol. Liq.* **2019**, *284*, 182–192.
6. Hsissou, R.; Abbout, S.; Safi, Z.; Benhiba, F.; Wazzan, N.; Guo, L.; Nouneh, K.; Briche, S.; Erramli, H.; Touhami, M.E.; et al. Synthesis and anticorrosive properties of epoxy polymer for CS in [1 M] HCl solution: Electrochemical, AFM, DFT and MD simulations. *Constr. Build. Mater.* **2021**, *270*, 121454.
7. van de Werken, N.; Tekinalp, H.; Khanbolouki, P.; Ozcan, S.; Williams, A.; Tehrani, M. Additively manufactured carbon fiber-reinforced composites: State of the art and perspective. *Addit. Manuf.* **2020**, *31*, 100962.
8. Asim, M.; Saba, N.; Jawaid, M.; Nasir, M.; Pervaiz, M.; Alothman, O.Y. A Review on Phenolic Resin and its Composites. *Curr. Anal. Chem.* **2018**, *14*, 185–197.
9. Hsissou, R.; Abbout, S.; Berisha, A.; Berradi, M.; Assouag, M.; Hajjaji, N.; Elharfi, A. Experimental, DFT and molecular dynamics simulation on the inhibition performance of the DGDCBA epoxy polymer against the corrosion of the E24 carbon steel in 1.0 M HCl solution. *J. Mol. Struct.* **2019**, *1182*, 340–351.
10. Hsissou, R.; Seghiri, R.; Benzekri, Z.; Hilali, M.; Rafik, M.; Elharfi, A. Polymer composite materials: A comprehensive review. *Compos. Struct.* **2021**, *262*, 113640.
11. Amrollahi, S.; Ramezanzadeh, B.; Yari, H.; Ramezanzadeh, M.; Mahdavian, M. Synthesis of polyaniline-modified graphene oxide for obtaining a high performance epoxy nanocomposite film with excellent UV blocking/anti-oxidant/ anti-corrosion capabilities. *Compos. Part B Eng.* **2019**, *173*, 106804.
12. Rod, K.A.; Nguyen, M.-T.; Elbakhshwan, M.; Gills, S.; Kutchko, B.; Varga, T.; McKinney, A.M.; Roosendaal, T.J.; Childers, M.I.; Zhao, C.; et al. Insights into the physical and chemical properties of a cement-polymer composite developed for geothermal wellbore applications. *Cem. Concr. Compos.* **2019**, *97*, 279–287.
13. Le Guen, M.J.; Newman, R.H.; Fernyhough, A.; Emms, G.W.; Staiger, M.P. The damping–modulus relationship in flax–carbon fibre hybrid composites. *Compos. B Eng.* **2016**, *89*, 27–33.
14. Nagarajan, B.; Arshad, M.; Ullah, A.; Mertiny, P.; Qureshi, A.J. Additive manufacturing ferromagnetic polymers using stereolithography—materials and process development. *Manuf. Lett.* **2019**, *21*, 12–16.
15. Nobile, M.R. Rheology of polymer–carbon nanotube composites melts. In *Polymer-Carbon Nanotube Composites: Preparation, Properties and Applications*; McNally, T., Pötschke, P., Eds.; Woodhead Publishing: Sawston, UK, 2011; pp. 428–481.
16. Zhou, W.; Kou, Y.; Yuan, M.; Li, B.; Cai, H.; Li, Z.; Chen, F.; Liu, X.; Wang, G.; Chen, Q.; et al. Polymer composites filled with core@double-shell structured fillers: Effects of multiple shells on dielectric and thermal properties. *Compos. Sci. Technol.* **2019**, *181*, 107686.
17. Asim, M.; Jawaid, M.; Nasir, M.; Saba, N. Effect of fiber loadings and treatment on dynamic mechanical, thermal and flammability properties of pineapple leaf fiber and kenaf phenolic composites. *J. Renew. Mater.* **2018**, *6*, 383–393.
18. Yavin, B.; Gallis, H.E.; Scherf, J.; Eitan, A.; Wagner, H.D. Continuous monitoring of the fragmentation phenomenon in single fiber composite materials. *Polym. Compos.* **1991**, *12*, 436–446.
19. Botelho, E.C.; Campos, A.N.; De Barros, E.; Pardini, L.C.; Rezende, M.C. Damping behavior of continuous fiber/metal composite materials by the free vibration method. *Compos. Part B Eng.* **2005**, *37*, 255–263.
20. Liao, K.; Schultesiz, C.R.; Hunston, D.L.; Brinson, L.C. Long-term durability of fiber-reinforced polymer-matrix composite materials for infrastructure applications: A review. *J. Adv. Mater.* **1998**, *30*, 3–40.
21. Guo, Y.; Xu, Y.; Wang, Q.; Dong, Q.; Yi, X.; Jia, Y. Enhanced lightning strike protection of carbon fiber composites using expanded foils with anisotropic electrical conductivity. *Compos. Part A Appl. Sci. Manuf.* **2019**, *117*, 211–218.

22. Zhang, H.; Guo, Y.; Zhang, X.; Wang, X.; Wang, H.; Shi, C.; He, F. Enhanced shielding performance of layered carbon fiber composites filled with carbonyl iron and carbon nanotubes in the koch curve fractal method. *Molecules* **2020**, *25*, 969.
23. Burnley, L.; Correia, G. Manipulating Fiber Orientation for the Reduction of Warpage in Carbon Fiber Composite Sandwich Panels. 2019. Available online: <https://digitalcommons.calpoly.edu/cgi/viewcontent.cgi?article=1228&context=matesp> (accessed on 18 July 2022).
24. Wu, T.; Tinkloh, S.; Tröster, T.; Zinn, W.; Niendorf, T. Measurement and analysis of residual stresses and warpage in fiber reinforced plastic and hybrid components. *Metals* **2021**, *11*, 335.
25. Kushch, V.I. Elastic equilibrium of spherical particle composites with transversely isotropic interphase and incoherent material interface. *Int. J. Solids Struct.* **2021**, *232*, 111180.
26. Kushch, V.I.; Sevostianov, I. Conductivity and elastic stiffness of spherical particle composite with partially disordered microstructure. *Int. Eng. Sci.* **2021**, *162*, 103473.
27. Staropoli, M.; Rogé, V.; Moretto, E.; Didierjean, J.; Michel, M.; Duez, B.; Steiner, P.; Thielen, G.; Lenoble, D.; Thomann, J.S. Hybrid silica-based fillers in nanocomposites: Influence of isotropic/isotropic and isotropic/anisotropic fillers on mechanical properties of styrene-butadiene (SBR)-based rubber. *Polymers* **2021**, *13*, 2413.
28. Liu, J.-T.; Xie, F.-Y.; He, Q.-C.; Tang, S.-L.; Xiao, C.-W. Effective elastic isotropic moduli of highly filled particulate composites with arbitrarily shaped inhomogeneities. *Mech. Mater.* **2019**, *135*, 35–45.
29. Lefèvre, V.; Lopez-Pamies, O. The effective shear modulus of a random isotropic suspension of monodisperse rigid n-spheres: From the dilute limit to the percolation threshold. *Extrem. Mech. Lett.* **2022**, *55*, 101818.
30. Lin, S.P.; Han, J.L.; Yeh, J.T.; Chang, F.C.; Hsieh, K.H. Composites of UHMWPE fiber reinforced PU/epoxy grafted interpenetrating polymer networks. *Eur. Polym. J.* **2007**, *43*, 996–1008.
31. Li, W.; Li, R.; Li, C.; Chen, Z.-R.; Zhang, L. Mechanical properties of surface-modified ultra-high molecular weight polyethylene fiber reinforced natural rubber composites. *Polym. Compos.* **2015**, *38*, 1215–1220.
32. Zheng, Z.; Tang, X.; Shi, M.; Zhou, G. Surface modification of ultrahigh-molecular-weight polyethylene fibers. *J. Polym. Sci. Part B Polym. Phys.* **2004**, *42*, 463–472.
33. Zhamu, A.; Wingert, M.; Jana, S.; Zhong, W.-H.; Stone, J.J. Treatment of functionalized graphitic nanofibers (GNFs) and the adhesion of GNFs-reinforced-epoxy with ultra high molecular weight polyethylene fiber. *Compos. Part A Appl. Sci. Manuf.* **2007**, *38*, 699–709.
34. Cartwright, B.K.; Mulcahy, N.L.; Chhor, A.O.; Thomas, S.G.; Suryanarayana, M.; Sandlin, J.D.; Crouch, I.G.; Naebe, M. Thermoforming and structural analysis of combat helmets. *J. Manuf. Sci. Eng.* **2015**, *137*, 051011.
35. Zhang, W.; Hu, Z.; Zhang, Y.; Lu, C.; Deng, Y. Gel-spun fibers from magnesium hydroxide nanoparticles and UHMWPE nanocomposite: The physical and flammability properties. *Compos. Part B Eng.* **2013**, *51*, 276–281.
36. Debnath, S.; Ranade, R.; Wunder, S.L.; Baran, G.R.; Zhang, J.; Fisher, E.R. Chemical surface treatment of ultrahigh molecular weight polyethylene for improved adhesion to methacrylate resins. *J. Appl. Polym. Sci.* **2005**, *96*, 1564–1572.
37. Voigt, W. Ueber die Beziehung zwischen den beiden Elasticitätsconstanten isotroper Körper. *Ann. Phys.* **1889**, *274*, 573–587. <https://doi.org/10.1002/andp.18892741206>.
38. Reuss, A. Berechnung der Fließgrenze von Mischkristallen auf Grund der Plastizitätsbedingung für Einkristalle. *Z. Angew. Math. Mech.* **1929**, *9*, 49–58. <https://doi.org/10.1002/zamm.19290090104>.
39. Yan, S.; Wang, B.; Sun, Y.; Lyu, B. Micromechanics-Based Prediction Models and Experimental Validation on Elastic Modulus of Recycled Aggregate Concrete. *Sustainability* **2021**, *13*, 11172.
40. Kulyk, V.; Duriagina, Z.; Kostryzhev, A.; Vasylyv, B.; Vavrukh, V.; Marenych, O. The Effect of Yttria Content on Microstructure, Strength, and Fracture Behavior of Yttria-Stabilized Zirconia. *Materials* **2022**, *15*, 5212.
41. Wang, M.; Hang, X. Modified Micro-Mechanics Based Multiscale Model for Damage Analysis of Open-Hole Composite Laminates under Compression. *Materials* **2022**, *15*, 5105.
42. Shan, M.; Zhao, L.; Ye, J. A Novel Micromechanics-Model-Based Probabilistic Analysis Method for the Elastic Properties of Unidirectional CFRP Composites. *Materials* **2022**, *15*, 5090.
43. Halpin, J.C.; Tsai, S.W. *Effects of Environmental Factors on Composite Materials*; AFML-TR; Air Force Materials Laboratory: Dayton, OH, USA, 1969; pp. 67–243.
44. Jones, R.M. *Mechanics of Composite Materials*; Hemisphere Publishing: New York, NY, USA, 1975; p. 115.
45. Michel, J.; Moulinec, H.; Suquet, P. Effective properties of composite materials with periodic microstructure: A computational approach. *Comput. Methods Appl. Mech. Eng.* **1999**, *172*, 109–143.
46. Yi, Y.-M.; Park, S.-H.; Yoon, S.-K. Asymptotic homogenization of viscoelastic composites with periodic microstructures. *Int. J. Solids Struct.* **1998**, *35*, 2039–2055.
47. Fujii, D.; Chen, B.C.; Kikuchi, N. Composite material design of two-dimensional structures using the homogenization design method. *Int. J. Numer. Methods Eng.* **2001**, *50*, 2031–2051.

48. Cadman, J.E.; Zhou, S.; Chen, Y.; Li, Q. On design of multi-functional microstructural materials. *J. Mater. Sci.* **2013**, *48*, 51–66.
49. Babu, K.P.; Mohite, P.M.; Upadhyay, C.S. Development of an RVE and its stiffness predictions based on mathematical homogenization theory for short fibre composites. *Int. J. Solids. Struct.* **2018**, *130*, 80–104.
50. Chen, X.; Wang, X.; Cao, C.; Yuan, Z.; Yu, D.; Li, F.; Chen, X. Elongational Flow Field Processed Ultrahigh Molecular Weight Polyethylene/Polypropylene Blends with Distinct Interlayer Phase for Enhanced Tribological Properties. *Polymers* **2021**, *13*, 1933.
51. Yun, J.-H.; Jeon, Y.-J.; Kang, M.-S. Prediction of the Elastic Properties of Ultra High Molecular-Weight Polyethylene Particle-Reinforced Polypropylene Composite Materials through Homogenization. *Appl. Sci.* **2022**, *12*, 7699.